Res Chem Intermed
DOI 10.1007/s11164-015-2304-y

# Synthesis, characterization, and catalytic application of Cr and Mn Schiff base complexes immobilized on modified nanoporous MCM-41

**Mohsen Nikoorazm[1] · Arash Ghorbani-Choghamarani[1] · Nourolah Noori[1]**

Received: 24 June 2015 / Accepted: 28 September 2015


**Abstract** Immobilization of chromium and manganese Schiff base complexes by postgrafting of ligand then metal salts on the walls of mesoporous MCM-41 functionalized with (3-aminopropyl)triethoxysilane is described. Characterization of the resulting heterogeneous catalysts by Fourier-transform infrared (FT-IR) spectroscopy, thermogravimetric analysis (TGA), transmission electron microscopy (TEM), X-ray diffraction (XRD) analysis, and Brunauer–Emmett–Teller (BET) techniques indicated successful grafting of these two complexes inside the nanochannels of MCM-41. The complexes were found to be efficient, selective catalysts for oxidation of various sulfides to sulfoxides and oxidative coupling of thiols to corresponding disulfides using $H_2O_2$ as oxidant at room temperature. The recycling results of these heterogeneous catalysts showed good recyclability without significant loss of activity or selectivity in successive runs, indicating that the Cr and Mn Schiff base complexes supported on nanoporous MCM-41 remained intact and the coordination environments were not altered during the reaction.

**Keywords** MCM-41 · Cr-MCM-41 · Mn-MCM-41 · Sulfoxide · Disulfide · Urea hydrogen peroxide (UHP)

## Introduction

Great interest has been shown in synthesis of Schiff bases and their transition-metal (V, Cr, Mn, Fe, etc.) complexes because of various applications such as metal chelating agents, heterogeneous and homogeneous catalysts, antimicrobial agents, pesticides, antitumor agents, spectrophotometric and fluorimetric agents, in

✉ Mohsen Nikoorazm
e_nikoorazm@yahoo.com

[1] Department of Chemistry, Faculty of Science, Ilam University, P.O. Box 69315516, Ilam, Iran

Published online: 23 October 2015

trace metal analysis, and in solar cells [1–5]. Among the above-mentioned applications, heterogeneous catalysts play an important role in chemical processes in industry [6, 7]. It is noted that application of homogeneous catalysts in chemical reactions is greatly limited due to high cost of recovery and lack of reusability. To heterogenize homogeneous catalysts, three general methods are available: (1) encapsulation in nanocavities of mesoporous material, for instance zeolites [8–10], (2) immobilization via covalent bonding with functionalized polymers [11, 12], MCM-41, or SBA-15 materials [13, 14], and (3) polymerization of the homogeneous catalyst itself [15–17], hence making them insoluble in solvents. Among these support materials, mesoporous silica MCM-41 has been employed as a useful and versatile solid support for preparation of heterogeneous catalysts, enzyme immobilization, and drug delivery because of its large tunable pore dimensions, high surface area, and great diversity in terms of surface functionalization. In the last decade, the immobilization strategy used for linking metal Schiff base complexes to supports to form heterogeneous catalysts has received wide attention in the catalyst field and industry [18–22]. Immobilization of homogeneous catalysts such as Schiff base complexes on MCM-41 yields specific additional characteristics such as selectivity, thermal stability, and easy separation from the reaction mixture and recyclability; For instance, copper and cobalt salen compounds have been grafted onto the surface of MCM-41 by means of aminosilane linkers via adduct formation, and these heterogeneous catalysts are considered to be active for oxidation reactions of sulfides to sulfoxides and conversion of thiols to disulfides under mild conditions in organic media [23, 24]. Considering the fact that thiols and sulfides are easily oxidizable and overoxidized, many studies have been conducted to devise methods to control oxidation of these compounds [25–28].

We report preparation and characterization of functionalized MCM-41 consisting of chromium and manganese Schiff base complexes retained on the internal surface of the nanoporous material using a postgrafting method. When using a direct co-condensation method, the amino-organosilanes are introduced into the mother gel with tetraethylorthosilicate (TEOS) simultaneously, leading to a homogeneous distribution of amino-organic moieties in the silica framework, though the presence of amino groups in the silica walls is unavoidable to some extent. On the other hand, in the postsynthesis grafting method, all amino-organic moieties introduced into the silica are anchored onto surface silanol groups via covalent bonds. This method may be advantageous when the goal is to maximize the number of amino groups on the surface. However, one disadvantage of the postsynthesis grafting method is that the distribution of the organic moiety on the surface is uncontrollable [29]. These immobilized complexes were used for oxidation reaction of various sulfides and oxidative coupling of thiols as active and reusable catalysts with high stability at room temperature. The effects of important reaction parameters such as the molar ratio of UHP to substrate, the nature of the solvent, and the amount of catalyst on the reactivity and selectivity were also examined. Finally, the reusability of the catalysts was studied.

## Experimental

### Techniques

Powder X-ray diffraction of Mn-MCM-41 and Cr-MCM-41 catalysts was carried out using a Philips diffractometer with Cu $K_\alpha$ radiation at 40 kV and 30 mA. The porosity and surface area of the samples were determine by the BET method using a BELSORP-MINI instrument. Fourier-transform infrared (FT-IR) spectra were recorded from KBr pellets using a Bruker VRTEX 70 FT-IR spectrometer. Transmission electron microscopy (TEM) images were taken using a Philips CM10 microscope at operating voltage of 200 kV. Ultraviolet–visible (UV–Vis) spectra were recorded on a PerkinElmer Lambda 20 UV–Vis spectrophotometer using barium sulfate as standard. Thermogravimetric analysis (TGA) of the samples was carried out between 30 and 900 °C in air at heating rate of 10 °C $min^{-1}$ using a Shimadzu DTG-60 automatic thermal analyzer.

## Materials

Tetraethylorthosilicate (TEOS, 98 %), cationic surfactant cetyltrimethylammonium bromide (CTAB, 98 %), chromium(III) chloride hexahydrate ($CrCl_3{\cdot}6H_2O$), manganous(II) chloride dihydrate ($MnCl_2{\cdot}2H_2O$), 3,4-dihydroxybenzaldehyde, aryl and alkyl sulfides, thiols, urea hydrogen peroxide (UHP), solvents, and other reagents were purchased from Merck, Aldrich or Fluka chemical companies and used as received without further purification.

### Synthesis of MCM-41 modified with (3-aminopropyl)triethoxysilane (3-APTES)

Synthesis of nanosized MCM-41 was carried out by the sol–gel method using cetyltrimethylammonium bromide (CTAB) as template, tetraethylorthosilicate (TEOS) as Si source, and sodium hydroxide as pH control agent. In a typical procedure, surfactant CTAB (2.74 mmol, 1 g) was added to a solution of deionized water (480 mL) and NaOH (2 M, 3.5 mL) at 80 °C. When the solution became homogeneous, TEOS (5 mL) was added dropwise to the solution under continuous stirring at 80 °C, and the obtained gel was aged under reflux for 2 h. The mixture was allowed to cool to room temperature, and the resulting product was filtered, washed with distilled water, then Soxhlet-extracted with ethanol for 24 h and dried in an oven at 60 °C. The obtained material was calcined at 550 °C in air for 5 h and designated MCM-41. Postsynthesis organic modification of MCM-41 was performed by stirring 1 g MCM-41 with a solution of 3-APTES in *n*-hexane (96 mL) at 80 °C for 24 h under nitrogen atmosphere. The resulting white solid of functionalized MCM-41 (APTES@MCM-41) was filtered, washed with *n*-hexane, and dried under vacuum [30].

### Preparation of heterogeneous catalyst Cr-Schiff base complex grafted on mesoporous silica MCM-41 (Cr-MCM-41)

For grafting of the ligand to MCM-41-($SiCH_2CH_2CH_2NH_2$)$_x$, a mixture of freshly dried APTES@MCM-41 (1 g) with 3,4-dihydroxybenzaldehyde (1 mmol, 0.134 g) in ethanol was refluxed under $N_2$ atmosphere for 3 h. Then, the resulting yellowish solid was filtered, washed with ethanol for several times, and dried at room temperature. Finally, a mixture of yellowish precipitate (1 g) and $CrCl_3{\cdot}6H_2O$ (0.13 mmol, 0.5 g) in ethanol was refluxed and mechanically stirred for 24 h at 80 °C. The resulting Cr-MCM-41 catalyst was filtered, washed with ethanol, and dried under vacuum (Scheme 1).

### Preparation of heterogeneous catalyst Mn(II)-Schiff base complex grafted on mesoporous silica (Mn-MCM-41)

To prepare silylated Mn-MCM-41, a mixture of the prepared yellowish precipitate (1 g) and $MnCl_2{\cdot}2H_2O$ (1 mmol, 0.161 g) in ethanol was refluxed and mechanically stirred at room temperature for 24 h. The resulting catalyst was filtered, washed with ethanol, and dried under vacuum.

### General procedure for oxidation of sulfides with UHP catalyzed by Cr-MCM-41 and Mn-MCM-41

To examine the catalytic activity of Cr-MCM-41 and Mn-MCM-41, we studied catalytic oxidation of several types of alkyl and aryl sulfides to corresponding sulfoxides at room temperature (Scheme 2). A mixture of sulfides (1 mmol), UHP (5 mmol), and Cr- or Mn-MCM-41 (25 mg) was stirred in ethanol at room temperature, and the progress of the reaction was monitored by thin-layer chromatography (TLC). After completion of the reaction, the catalyst was separated

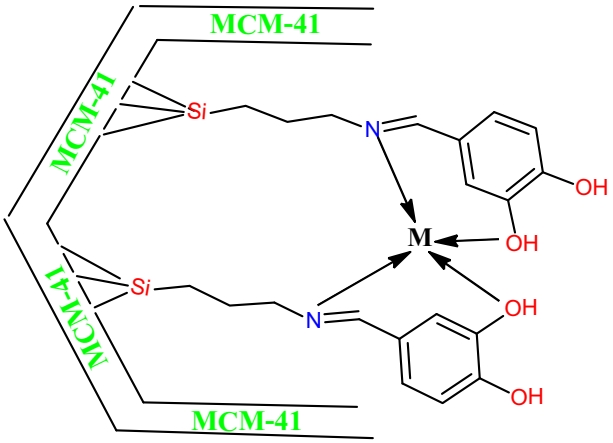


**Scheme 1** Schematic representation of synthesis of heterogeneous catalyst M-MCM-41 (M = Cr or Mn)

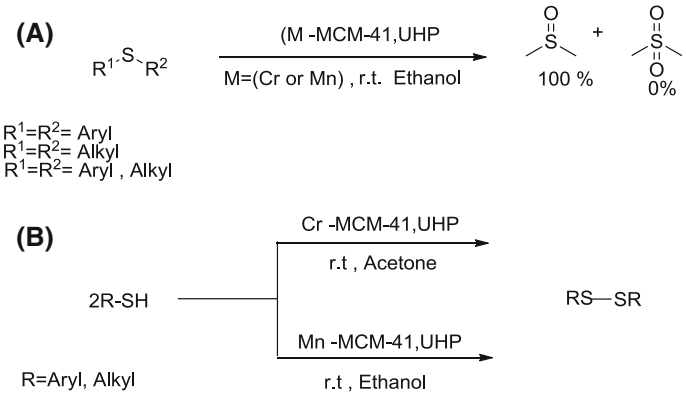


**Scheme 2** Selectivity in **a** oxidation of sulfides and **b** oxidative coupling of thiols by present procedure

by simple filtration and washed with dichloromethane (3 × 10 mL). The results are presented in Table 4.

### General procedure for oxidative coupling of thiols to disulfides with UHP catalyzed by Cr-MCM-41 and Mn-MCM-41

Thiols ((1 mmol), 5 mmol UHP, and 4 mL acetone as solvent along with 25 mg catalyst were added to a 10-mL two-necked flask equipped with a stirrer. The progress of the reaction was monitored by TLC. After completion of the reaction, the catalyst was removed and the pure products were extracted with $CH_2Cl_2$ (3 × 10 mL). The results are presented in Table 6.

## Results and discussion

### XRD analysis

The low-angle XRD patterns of MCM-41, MCM-41-$NH_2$, MCM-41-ligand, Cr-MCM-41, and Mn-MCM-41 are shown in Fig. 1. The XRD pattern of MCM-41 shows a typical three-peak pattern with very strong reflection at $2\theta = 2.41°$ for $d_{100}$ and also two other weaker reflections at $2\theta = 3.95°$ and 4.55° for $d_{110}$ and $d_{200}$, respectively, which can be attributed to formation of well-ordered mesoporous material with hexagonal symmetry. All peaks are well resolved, indicating good-quality material. Comparison of the XRD patterns for MCM-41 and Cr-MCM-41 shows that, upon postsynthetic grafting, the $d_{110}$ and $d_{200}$ reflections were no longer observed and an overall decrease in the intensity of $d_{100}$ was observed. This result can be attributed to decrease of local order, such as variation in wall thickness, or might be due to reduction of scattering between the channel walls of the silicate framework and the Schiff base ligand present in Cr-MCM-41, as mentioned previously [31]. The values of the unit cell parameter $a_0 = (2/\sqrt{3})d_{100}$ are 27.86

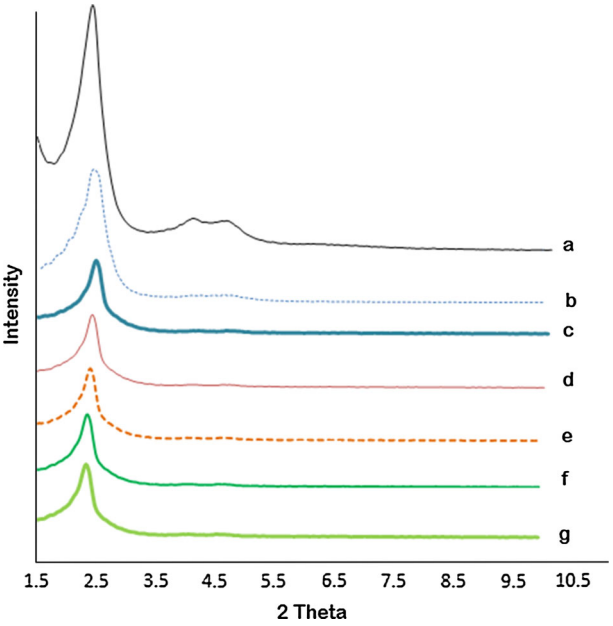


**Fig. 1** XRD patterns: *a* MCM-41, *b* MCM-41-$NH_2$, *c* MCM-41-ligand, *d* Cr-MCM-41, *e* Mn-MCM-41, *f* recovered Cr-MCM-41, and *g* recovered Mn-MCM-41

and 31.32 Å for MCM-41 and Cr-MCM-41, respectively. The increase in the lattice parameter of Cr-MCM-41 is due to the functionalization of MCM-41. Similarly, Mn-MCM-41 and recycled Mn-MCM-41 prepared by the postsynthesis procedure exhibited XRD patterns akin to those shown in Fig. 1. Obviously, upon postgrafting of Cr and Mn Schiff base complexes, well-defined (100) reflections are observed in the XRD patterns, but there are no well-resolved (110, 200) peaks, which are clearly visible from corresponding MCM-41 analogs; the intensity of the peak at $d_{100}$ decreased with increasing loading amount of Cr and Mn, indicating that the hexagonal mesostructure was less ordered due to successful introduction of Cr and Mn metal elements into the mesoporous channels of MCM-41. Also, the structural stability of the samples was retained after grafting of the organometallic complexes.

## $N_2$ adsorption–desorption studies

The $N_2$ adsorption–desorption isotherms of MCM-41, functionalized MCM-41, Cr-MCM-41, and Mn-MCM-41 are shown in Fig. 2. According to the International Union of Pure and Applied Chemistry (IUPAC) classification characteristics for mesoporous structures, the isotherms of all samples show a type IV curve and a hysteresis loop resulting from capillary condensation of $N_2$ gas inside mesopores [32]. In comparison with the parent MCM-41, the relative pressure is transformed to a lower value for the modified samples, leading to a reduction of the BET specific area, pore volume, and pore diameter. These results are presented in Table 1. These

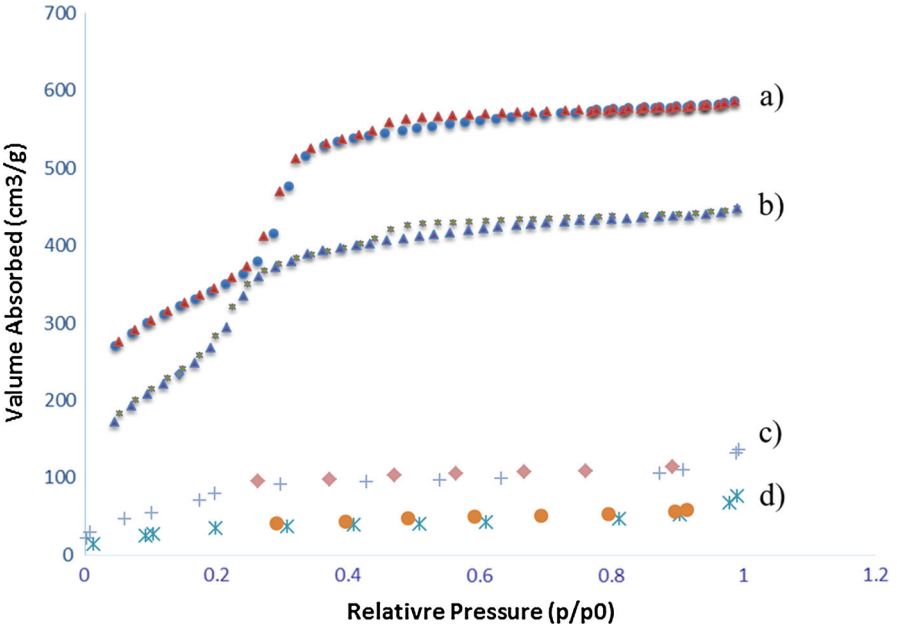


**Fig. 2** $N_2$ adsorption–desorption isotherms for *a* MCM-41, *b* MCM-41-$NH_2$, and *c* Cr-MCM-41 and Mn-MCM-41

**Table 1** Surface properties of MCM-41, MCM-41-$NH_2$, Cr-MCM-41, and Mn-MCM-41

| Sample | $S_{BET}$ ($m^2$/g) | Pore diam. by BJH method (nm) | Pore vol. ($cm^3$/g) | Wall diam. (nm) |
|---|---|---|---|---|
| MCM-41 | 986.16 | 3.65 | 0.711 | 0.902 |
| MCM-41-$NH_2$ | 694.98 | 3.3 | 0.340 | 0.906 |
| Cr-MCM-41 | 311.39 | 1.2 | 0.205 | 1.93 |
| Mn-MCM-41 | 130.12 | 1.1 | 0.116 | 2.02 |

results confirm good grafting of the transition-metal complexes into the MCM-41 channels. The $N_2$ adsorption–desorption analysis of Cr-MCM-41 and Mn-MCM-41 gave typical type IV adsorption isotherms with a H1 hysteresis loop according to the IUPAC classification, indicating presence of mesoporosity. As shown in Table 1, the surface area and specific pore volume of Cr-MCM-41, Mn-MCM-41, and functionalized MCM-41 with amino group decreased notably compared with MCM-41. The sorption experiment yielded a BET pore volume of 0.711 $cm^3\ g^{-1}$ and surface area of 986.16 $m^2\ g^{-1}$ for MCM-41, while postgrafting of amino group, chromium and manganese Schiff base complexes remarkably reduced the surface area compared with MCM-41. In addition, the pore diameter reduced from 3.56 nm for pure silica MCM-41 to 1.2 and 1.1 nm for Cr-MCM-41 and Mn-MCM-41, respectively. On the other hand, an increase of the wall thickness occurred, which is in agreement with anchoring of functionalized groups onto MCM-41, based on

which it can be concluded that the chromium and manganese Schiff base complexes occur inside the channels.

## Fourier-transform infrared (FT-IR) spectroscopy

Infrared spectroscopy was used as a key method to characterize the functional groups of the products (Fig. 3). The FT-IR spectrum of MCM-41 shows three peaks at 1083, 793, and 463 $cm^{-1}$, corresponding to asymmetric stretching, symmetric stretching, and bending Si–O–Si vibration, respectively. The presence of the peak at around 1550 $cm^{-1}$, mainly from $NH_2$ symmetric bending vibration, indicates successful grafting of organic amine onto the MCM-41 surface. The free ligand exhibits a $\nu$(C=N) stretch at 1657 $cm^{-1}$, while in Cr-MCM-41 and Mn -MCM-41 this band shifts to lower frequency and appears at 1638 and 1641 $cm^{-1}$, respectively. The spectra for recycled Cr-MCM-41 and Mn-MCM-41 point out that the catalysts were stable during the reaction.

## TEM analysis

TEM micrographs showing top (A) and side (B) views of MCM-41 are presented in Fig. 4. The regular arrangement of pores can be clearly observed for this material,

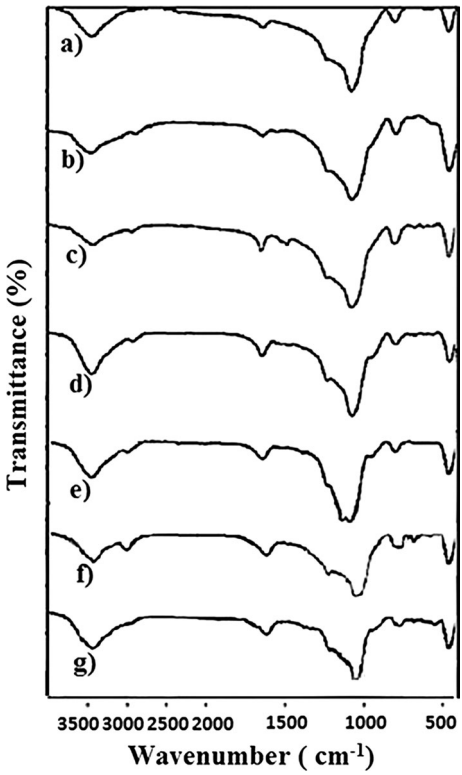


**Fig. 3** FT-IR spectra of *a* MCM-41, *b* MCM-41-$NH_2$, *c* MCM-41-ligand, *d* Cr-MCM-41, *e* recycled Cr-MCM-41, *f* Mn-MCM-41, and *g* recycled Mn-MCM-41

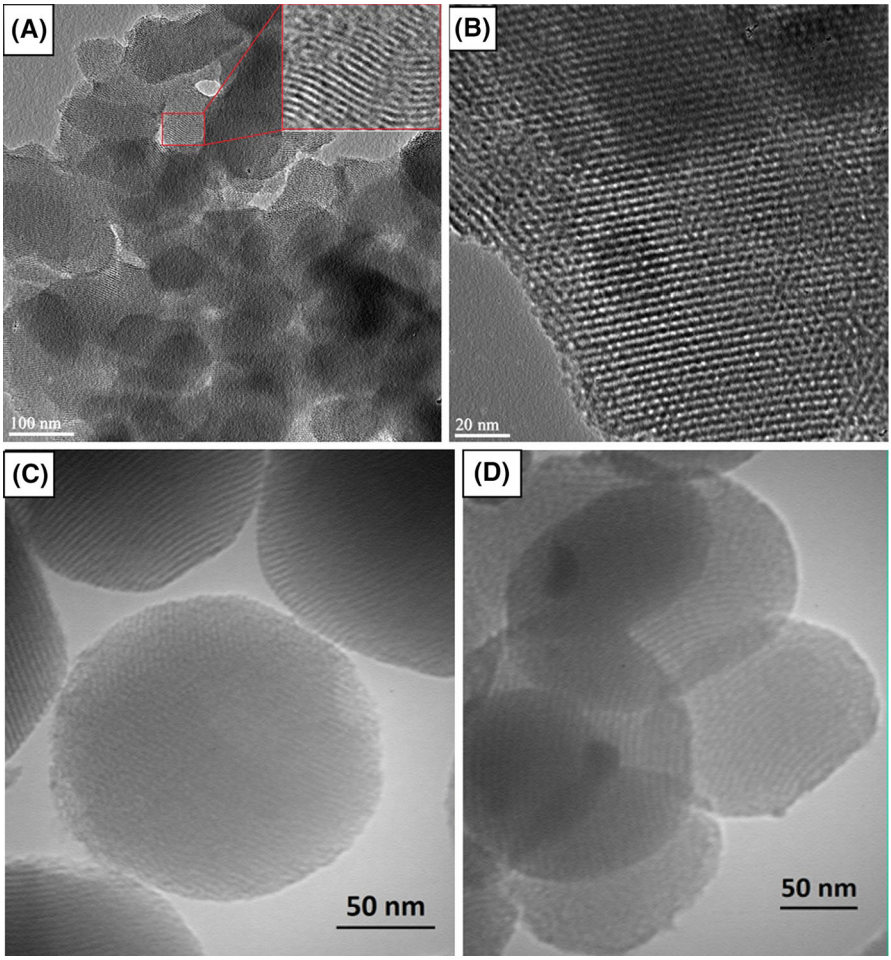


**Fig. 4** TEM images of MCM-41: **a** top view, **b** side view, and **c** Cr-MCM-41 and Mn-MCM-41

and also the hexagonal pores remained intact. Also Fig. 4 shows TEM images for Cr-MCM-41 and Mn-MCM-41. TEM observation of Cr-MCM-41 (Fig. 4c) indicated well-ordered hexagonal arrays of mesopores and long-range mesoporous architecture (50 nm). The Mn-MCM-41 sample also exhibited a similar type of array of regular hexagonal arrangement in TEM micrographs (Fig. 4d). Therefore, it can be concluded that both samples had a similar type of morphology.

## SEM analysis

The morphologies of MCM-41, Cr-MCM-41, and Mn-MCM-41 are shown in Fig. 5. As seen in the SEM images of Fig. 6, MCM-41, Cr-MCM-41, and Mn-MCM-41 are agglomerations of small spherical regular particles. As can be seen,

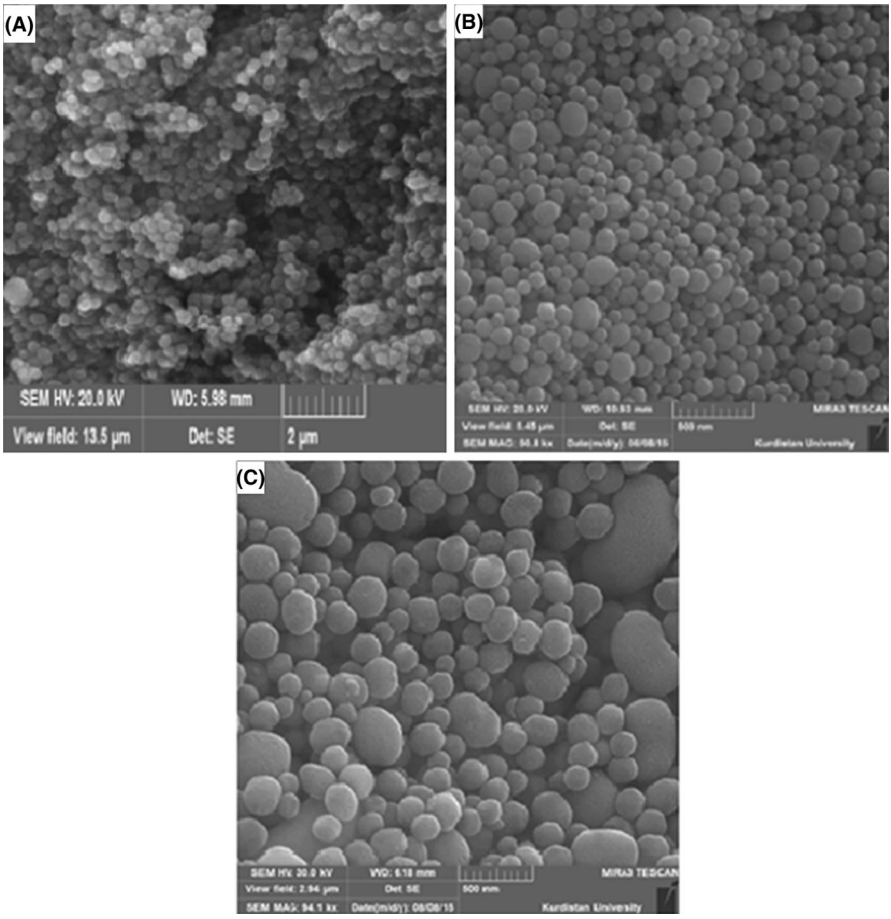


**Fig. 5** SEM images: **a** MCM-41, **b** Cr-MCM-41, and **c** Mn-MCM-41

there is no difference in the particle surface morphology between MCM-41 and the other materials, indicating that the Cr and Mn Schiff base complexes are supported inside the channels of MCM-41.

## Thermogravimetric analysis

The immobilization of the Schiff base complexes on the functionalized mesopores and the percentage of chemisorbed organic functional groups on MCM-41 can be studied based on TGA curves. The thermogravimetric (TG) analysis of the samples is shown in Fig. 6. TGA of the synthesized MCM-41 indicated 4.16 % mass loss in one step at 25–120 °C due to desorption of water [32]. The thermogram of amino-functionalized MCM-41 indicated a slow weight loss up to 840 °C. The TGA curve for MCM-41-$(SiCH_2CH_2CH_2NH_2)_x$ indicated four steps of weight loss (25–120, 120–340, 340–600, and >600 °C). The weight loss is 3 % in the first step, being due

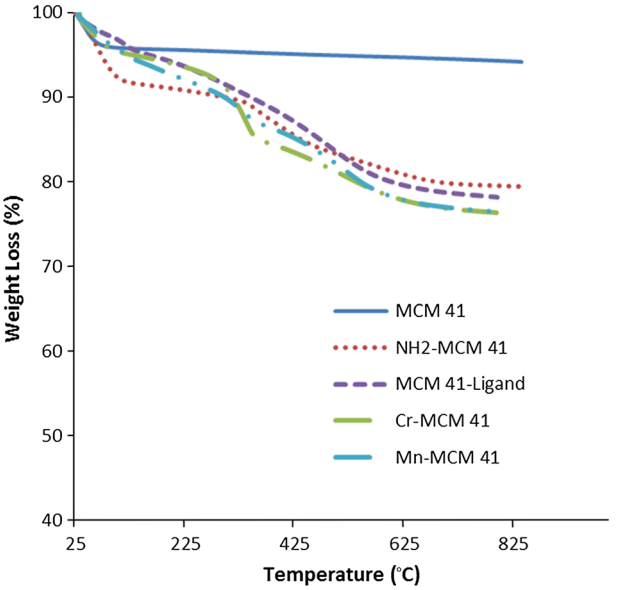


**Fig. 6** TG profiles for MCM-41 (*solid line*), MCM-41-$NH_2$, (*dotted line*), MCM-41-ligand (*dashed line*), Cr-MCM-41 (*dashed dotted line*), and Mn-MCM-41 (*dashed double-dotted line*)

**Table 2** TGA data of catalysts

| Catalyst | Temperature (°C) | Weight loss (%) | Group lost |
|---|---|---|---|
| Cr-MCM-41 | 25–100 | 4.5 | $H_2O$ |
| | 250–350 | 6 | Combustion of amine |
| | 450–600 | 7 | Decomposition of Schiff base |
| Mn-MCM-41 | 25–150 | 6 | $H_2O$ |
| | 280–350 | 7 | Combustion of amine |
| | 450–600 | 9 | Decomposition of Schiff base |

to removal of physically adsorbed water inside MCM-41 channels. The weight losses in the second and third steps (8 %) are chiefly related to oxidative decomposition of organic functional groups. In the final step, the third weight loss (1.67 %) is due to dehydroxylation of the silicate network, and the TGA curve of the MCM-41-ligand shows 13 % weight loss above 350 °C, chiefly associated with decomposition of organic groups. Based on elemental analysis, the amount of functional groups of APTES and ligand were computed to be 1.2 and 0.5 mmol $g^{-1}$ of MCM-41, respectively. The TGA data for the catalysts are presented in Table 2. The TGA curve of Cr- or Mn-salen-MCM-41 shows three stages of weight loss, confirming the formation of the Schiff base complexes.

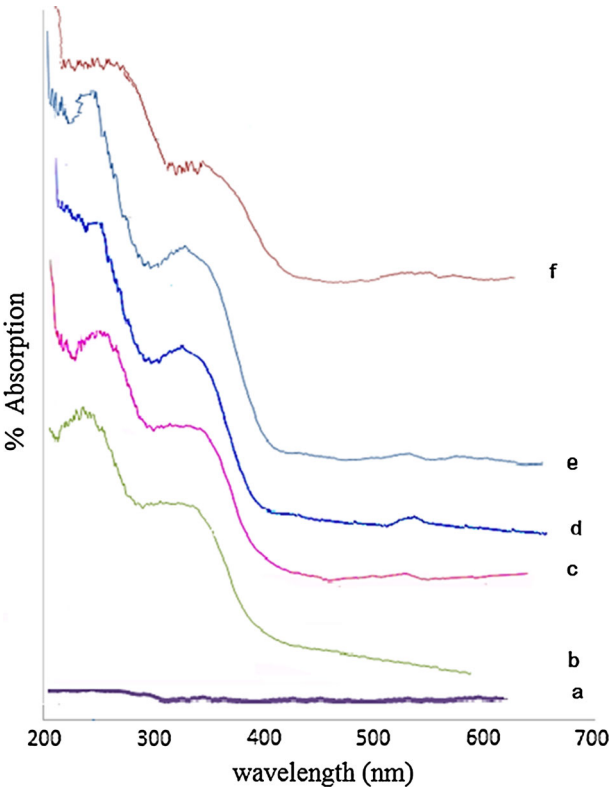


**Fig. 7** UV–Vis diffuse-reflectance spectra of *a* MCM-41, *b* MCM-41-ligand, *c* Cr-MCM-41, *d* Cr-MCM-41, *e* chromium Schiff base complex, and *f* manganese Schiff base complex

## UV–Vis spectroscopy

Figure 7 shows the UV–Vis diffuse-reflectance spectra of the samples. The UV–Vis spectra of the homogeneous complexes all displayed characteristic peak at 380–450 nm typical of metal–ligand band, and one weak broad peak at about 530–610 nm associated with *d*–*d* transitions. The UV–Vis spectra of all the immobilized complexes were quite similar to those of their corresponding homogeneous complexes.

In continuation of our previous work on organic transformation reactions [25, 34–36], we also studied here the application of the Mn or Cr Schiff base complexes supported on the modified nanoporous MCM-41 as heterogeneous and recoverable catalysts in oxidation reactions of sulfides to sulfoxides and oxidative coupling of thiols to corresponding disulfides using UHP as oxidizing agent (Scheme 2).

## Oxidation of sulfides to sulfoxides with UHP catalyzed by Cr-MCM-41 and Mn-MCM-41

To determine the optimum reaction conditions, dibenzyl sulfide was selected as a model substrate and oxidation of this substrate in various solvents was studied.

**Table 3** Oxidation of dibenzyl sulfide with UHP as oxidant in presence of Cr- or Mn-MCM-41 catalyst in different solvents

| Entry | Solvent | Time (h) | | Yield (%) | |
|---|---|---|---|---|---|
| | | Cr-MCM-41 | Mn-MCM-41 | Cr-MCM-41 | Mn-MCM-41 |
| 1 | Ethanol | 2 | 2.5 | 95 | 93 |
| 2 | Water | 10 | No reaction[a] | 91 | – |
| 3 | *n*-Hexane | 4.5 | 8 | 93 | 92 |
| 4 | Acetonitrile | 6 | 7 | 95 | 90 |
| 5 | Dichloromethane | 9 | 15 | 91 | 89 |
| 6 | Ethyl acetate | 11 | 18 | 90 | 88 |
| 7 | Acetone | 3.75 | 7.25 | 87 | 85 |

Reaction conditions: 1 mmol dibenzyl sulfide, 0.025 g catalyst, 5 mmol UHP in 4 mL solvent at room temperature

[a] After 24 h

Ethanol proved to be the optimum solvent (Table 3, entry 1) and was used in subsequent optimization studies. When oxidation of dibenzyl sulfide (1 mmol) was carried out using different concentrations of UHP, the reaction did not reach completion when using less than 5 mmol UHP. However, when a higher concentration (7 mmol) was employed, neither the conversion nor selectivity of the reaction was improved.

We also examined oxidation of dibenzyl sulfide (1 mmol) using UHP (5 mmol) in the absence of Cr- or Mn-MCM-41 catalyst at room temperature. It was observed that the reaction was completed after 12 h. However, when similar oxidation was conducted in the presence of the mentioned catalysts (25 mg) at room temperature (Fig. 8), dibenzyl sulfoxide was formed in excellent yield in short period of time. Based on the above observations, 1 mmol substrate, 5 mmol UHP, 25 mg catalyst,

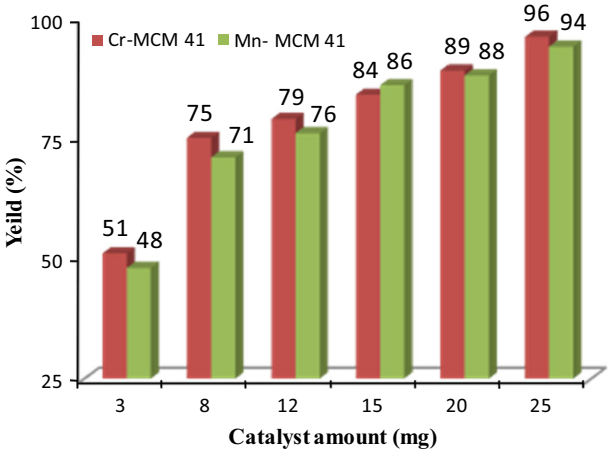


**Fig. 8** Effect of amount of catalysts in oxidation reaction of dibenzyl sulfide to sulfoxide

**Table 4** Oxidation of various sulfides with UHP catalyzed by Cr-MCM-41 and Mn-MCM-41 in ethanol ($R^1-S-R^2 \rightarrow R^1(S=O)-R^2$)

| Entry | $R_1$ | $R_2$ | Time (h) | | Yield[a] % | | M.p. (°C) | |
|---|---|---|---|---|---|---|---|---|
| | | | Cr-MCM-41 | Mn-MCM-41 | Cr-MCM-41 | Mn-MCM-41 | Cr-MCM-41 | Mn-MCM-41 |
| 1 | Ph | $CH_2CH_2OH$ | 23 | 27 | 95 | 94 | 148–149 | 147–149 [36] |
| 2 | $PhCH_2$ | $PhCH_2$ | 2 | 2.5 | 96 | 94 | 132–134 | 133–134 [36] |
| 3 | Ph | Ph | 7 days | 10 days | 93 | 90 | 69–70 | 68–70 [36] |
| 4 | Ph | $PhCH_2$ | 18 | 22 | 95 | 95 | 121–122 | 120–122 [36] |
| 5 | $C_{12}H_{25}$ | $C_{12}H_{25}$ | 8 | 12 | 97 | 96 | 88–90 | 88–90 [38] |
| 6 | $CH_3CH_2$ | $CH_3CH_2$ | 1.5 | 2.25 | 94 | 92 | 103–104 | 102–104 [37] |
| 7 | Furan | Furan | 2.25 | 4.30 | 93 | 95 | 83–85 | 83–85 [39] |
| 8 | Furyl | $CH_3$ | 0.33 | 0.5 | 95 | 93 | Oil | Oil [40] |
| 9 | $PhCH_2$ | $CH_3$ | 1 | 4 | 96 | 95 | Liq | Liq [41] |
| 10 | Ph | $CH_3$ | 8.75 | 11 | 95 | 92 | 30–31 | 29–31 [36] |
| 11 | Tetrahydrothiophene | – | 0.75 | 1.25 | 97 | 96 | 106–109 | 106–109 [42] |
| 12 | $CH_3$ | $CH_2CH_2COOCH_3$ | 2.5 | 3 | 92 | 91 | Liq | Liq [41] |

Reaction conditions: substrate (1 mmol), UHP (5 mmol), 25 mg catalyst in 4 mL ethanol at room temperature

[a] Isolated yield

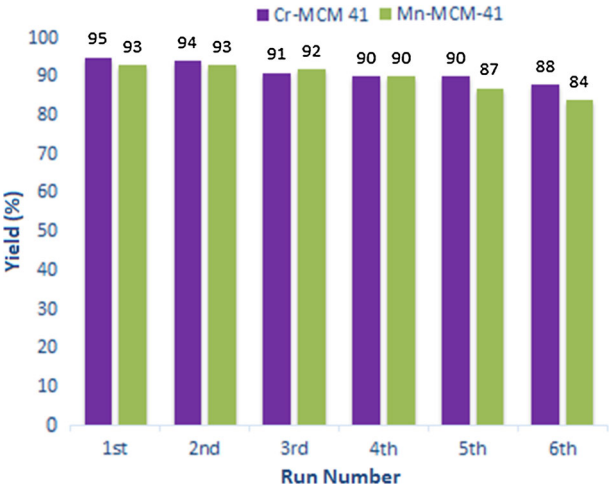


**Fig. 9** Recycling experiment of Cr-MCM-41 and Mn-MCM-41 for oxidation of dibenzyl sulfide

**Table 5** Oxidative coupling of 4-methylthiophenol using Cr- or Mn-MCM-41 and UHP in different solvents

| Entry | Solvent | Time (h) | | Yield (%) | |
|---|---|---|---|---|---|
| | | Cr-MCM-41 | Mn-MCM-41 | Cr-MCM-41 | Mn-MCM-41 |
| 1 | Ethanol | 2.5 | 0.33 | 93 | 96 |
| 2 | Water | 12 | 18 | 89 | 83 |
| 3 | *n*-Hexane | 4 | 9 | 92 | 90 |
| 4 | Acetonitrile | 17 | 1.25 | 90 | 94 |
| 5 | Dichloromethane | 6.25 | 15 | 92 | 91 |
| 6 | Acetone | 0.6 | 5.5 | 97 | 88 |
| 7 | Ethyl acetate | 3.45 | 6.5 | 92 | 90 |

Reaction conditions: 1 mmol 4-methylthiophenol, 0.02 g catalyst, 5 mmol UHP in 4 mL solvent at room temperature

and ethanol as solvent was the best combination for oxidation of sulfides to sulfoxides. To determine the general scope of this method, a wide range of sulfides were subjected to oxidation under the optimized condition. All the reactions occurred with high selectivity for sulfoxide formation, and no overoxidation products such as sulfone were detected in the reaction mixture (Table 4).

Finally, the reusability of Cr-MCM-41 and Mn-MCM-41 was investigated. After the reaction reached completion, catalyst was easily separated from the product using simple filtration, washed with ethanol and water, then reused in the next run. Figure 9 shows the yield of six consecutive cycles of the oxidation reaction of dibenzyl sulfide as model substrate.

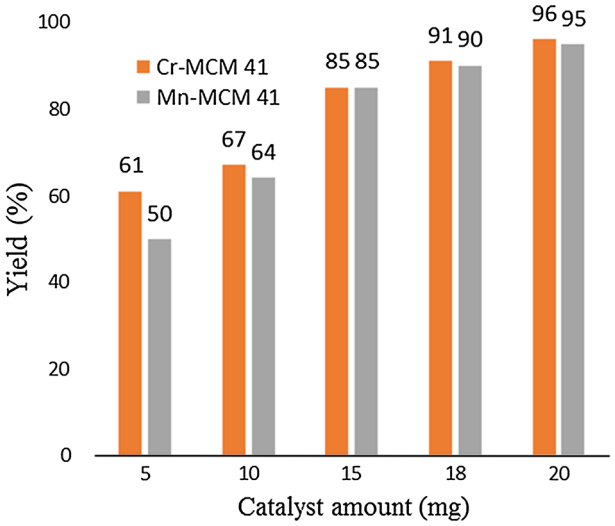


**Fig. 10** Effect of catalyst loading in oxidative coupling of thiol to disulfide

**Table 6** Oxidation of various thiols using UHP catalyzed by Cr-MCM-41 or Mn-MCM-41 (**R−SH→R−S−R**)

| Entry | R | Time (min) | | Yield[a] (%) | | M.p. (°C) | |
|---|---|---|---|---|---|---|---|
| | | Cr-MCM-41 | Mn-MCM-41 | Cr-MCM-41 | Mn-MCM-41 | Cr-MCM-41 | Mn-MCM-41 |
| 1 | *p*-$MeC_6H_4$– | 6 | 20 | 96 | 94 | 41–43 | 42–43 [44] |
| 2 | –$CH_2COOH$ | 36 | 15 | 93 | 93 | Oil | Oil [44] |
| 3 | 2-Naphthyl | 35 | 60 | 92 | 93 | 142–144 | 142–144 [44] |
| 4 | 2,6-$DiClC_6H_3$– | 32 | 24 | 89 | 95 | 76–90 | 76–90 [44] |
| 5 | *p*-$BrC_6H_4$– | 24 | 18 | 91 | 92 | 90–92 | 91–92 [45] |
| 6 | 2-Pyridyl– | 4 | 10 | 94 | 91 | 55–56 | 54–56 [46] |
| 7 | $C_6H_5$– | 39 | 75 | 90 | 90 | 55–57 | 56–57 [42] |
| 8 | 2-$COOHC_6H_4$– | 14 | 16 | 93 | 94 | 276–282 | 276–282 [44] |
| 9 | 2-Benzoxazole | 93 | 38 | 91 | 92 | 85–89 | 87–89 [44] |
| 10 | 2-Benzothiazole | 31 | 27 | 95 | 94 | 176–178 | 175–178 [44] |
| 11 | $HOCH_2CH_2$– | 21 | 27 | 94 | 89 | Oil | Oil [42] |

Reaction conditions: substrate (1 mmol), UHP (5 mmol), 20 mg catalyst Cr-MCM-41 with acetone solvent or Mn-MCM-41 with ethanol solvent

[a] Isolated yield

## Oxidative coupling of thiols to disulfides with UHP catalyzed by Cr-MCM-41 and Mn-MCM-41

To indicate the role of Cr-MCM-41 and Mn-MCM-41 as catalyst in the oxidative coupling of thiol reactions, the effects of various reaction parameters such as solvent,

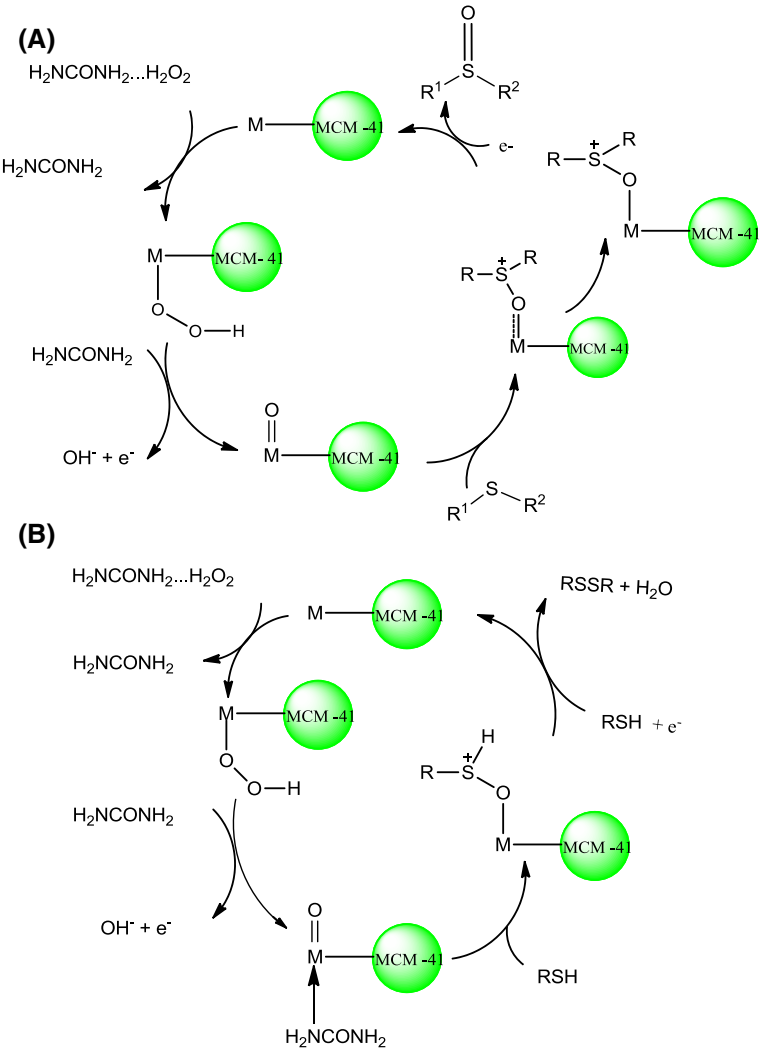


**Scheme 3** Proposed mechanism of **a** oxidation of sulfide and **b** oxidative coupling of thiol in presence of the synthesized catalysts

amount of catalyst, and substrate–oxidant ratio were studied to optimize the reaction conditions. Optimization experiments were carried out using 4-methylthiophenol as substrate. Among the different solvents listed in Table 5, ethanol and acetone were chosen as the best solvent for Cr-MCM-41 and Mn-MCM-41, respectively.

We loaded various amounts of the chosen catalysts in this reaction. The resulting optimized reaction condition for catalyst loading was 20 mg for Mn- or Cr-MCM-41. When the amount of catalyst was increased from 10 to 20 mg, the conversion increased from 64 to 95 % (Fig. 10).

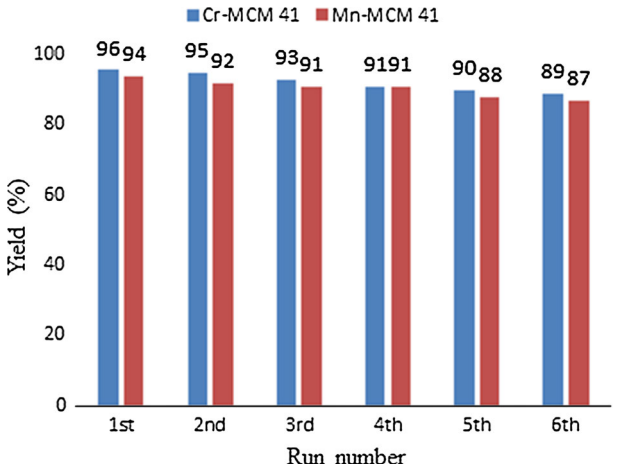


**Fig. 11** Reusability of Cr-MCM-41 or Mn-MCM-41 as catalysts in oxidative coupling of 4-methylthiophenol

The reaction rate as well as product yield was also found to depend on the oxidant concentration. It was seen that 5 mmol UHP was required to obtain disulfide selectivity with 1 mmol of substrate. The system with Cr- or Mn-MCM-41 and UHP as oxidizing agent was further extended to oxidation of various thiols (Table 6).

The active oxygen of UHP oxidizes RSH to RSOH, which reacts with another RSH molecule to produce disulfide. The proposed mechanism of oxidation of sulfide [47] and oxidative coupling [48] of thiol in presence of Cr-MCM-41 and Mn-MCM-41 by UHP as oxidant is displayed in Scheme 3.

To study the stability of the immobilized catalysts, 4-methylthiophenol was selected as a model substrate. The catalyst could be easily recovered after the reaction by simple filtration. After recovery, the catalysts were thoroughly washed with ethanol and then water, dried, and reused for subsequent experiments (six runs) by adding fresh substrate and oxidant under similar reaction conditions. In all cases, reaction times and yields of the desired product remained almost the same, establishing the recyclability and reusability of the immobilized Mn- and Cr-Schiff base complexes (Fig. 11).

## Conclusions

Chromium and manganese Schiff base complexes consisting of mesoporous material were synthesized by means of a postgrafting procedure and characterized using several techniques. Application of Cr-MCM-41 and Mn-MCM-41 as adequate and heterogeneous catalysts for synthesis of several sulfoxides and disulfides under mild conditions has been shown. The readiness of the catalyst synthesis, environmental friendliness, mild reaction conditions, and efficient recycling are among the other important benefits of this procedure.

**Acknowledgments** This work was supported by the research facilities of Ilam University, Ilam, Iran.

## References

1. G.S. Mishra, A. Kumar, Kinet. Catal. **394**, 45 (2004)
2. S. Nursen, P. Nihat, O. Hatice, K. Nurdan, Med. Chem. Res. **580**, 22 (2013)
3. Z.H. Chohana, S.H. Sumrraa, M.H. Youssoufib, T.B. Hadda, J. Coord. Chem. **3981**, 63 (2010)
4. M.N. Dehkordi, A.K. Bordbar, M.A. Mehrgardi, V. Mirkhani, J. Fluoresc. **1649**, 21 (2011)
5. J.B. Xia, H. Yang, F.Y. Li Huang, C.H. Huang. Chem J. Chin. U **204**, 27 (2006)
6. M. Beller, K. Kuhlein, Synlett **441**, 5 (1995)
7. P. Barbaro, F. Liguori, N. Linares, C.M. Marrodan, Eur. J. Inorg. Chem. **3807**, 243 (2012)
8. A. Mobinikhaledi, M. Zendehdel, P. Safari, J. Porous Mater. **565**, 21 (2014)
9. X. F. Zhou, J. Appl. Polym. Sci. **131**, 40809 (2014)
10. A. Okemoto, Y. Inoue, K. Ikeda, C. Tanaka, K. Taniya, Y. Ichihashi, S. Nishiyama, Chem. Lett. **1734**, 43 (2014)
11. E. Gross, F.D. Toste, G.A. Somorjai, Catal. Lett. **126**, 145 (2015)
12. X.L. Zeng, S. Yu, L. Ye, M.Y. Li, Z.L. Pan, R. Sun, B. Xu, J. Mater. Chem. **187**, 3 (2015)
13. C.N. Rohitha, S.J. Kulkarni, N. Narendar, Synth. Commun. **2853**, 43 (2013)
14. H. Chen, S. Kuranari, T. Akiyama, J.L. Zhang, M. Anpo, J. Catal. **215**, 257 (2008)
15. G. Marinescu, A.M. Madalan, M. Andruh, J. Coord. Chem. **479**, 68 (2015)
16. A.M. Bohnsack, I.A. Ibarra, V.I. Bakhmutov, V.M. Lynch, S.M. Humphrey, J. Am. Chem. Soc. **16038**, 135 (2013)
17. X. Jiang, Z.J. Li, Y.Y. Zhai, G. Yan, H. Xia, Z.H. Li, Cryst. Eng. Commun. **805**, 16 (2014)
18. X. Yuan, G.F. Shan, L.X. Li, J. Wu, H.A. Luo, Catal. Lett. **868**, 145 (2015)
19. M.T. Goldani, A. Mohammadi, R. Sandaroos, J. Chem. Sci. **801**, 126 (2014)
20. U.G. Singh, R.T. Williams, K.R. Hallam, G.C. Allen, J. Solid State Chem. **3405**, 178 (2005)
21. C. Gonzalez-Arellano, A. Corma, M. Iglesias, F. Sanchez, Adv. Synth. Catal. **1758**, 346 (2004)
22. M. Masteri-Farahani, F. Farzaneh, M. Ghandi, J. Mol. Catal. A-Chem. **53**, 248 (2006)
23. H. Chen, Y. Wang, Ceram. Int. **28**, 541–547 (2002)
24. V. Ayala, A. Corma, M. Iglesias, F. Sanchez, J. Mol. Catal. A: Chem. **201**, 221 (2004)
25. M. Nikoorazm, A. Ghorbani-Choghamarani, F. Ghorbani, H. Mahdavi, Z. Karamshahi. J. Porous Mater. **261**, 22 (2015)
26. B. Li, S. Bai, P. Wang, H. Yang, Q. Yangm, C. Li, Phys. Chem. Chem. Phys. **2504**, 13 (2011)
27. M. Bagherzadeh, L. Tahsini, R. Latifi, Catal. Commun. **1600**, 9 (2008)
28. M. Bagherzadeh, M. Amini, Inorg. Chem. Commun. **21**, 12 (2009)
29. T. Yokoi, H. Yoshitake, T. Tatsumi, J. Mater. Chem. **951**, 14 (2004)
30. F. Havasi, A. Ghorbani-Choghamarani, F. Nikpour, New J. Chem. **6504**, 39 (2015)
31. S. Bhunia, D. Saha, S. Koner, Langmuir **15322**, 27 (2011)
32. C.M. Kowalchuk, G. Schmid, W. Meyer-Zaika, Y. Huang, J.F. Corrigan, Inorg. Chem. **173**, 43 (2004)
33. M. Hajjami, F. Ghorbani, F. Bakhti, Appl. Catal. A-Gen. **303**, 470 (2014)
34. M. Nikoorazm, A. Ghorbani-Choghamarani, H. Mahdavi, S.M. Esmaeili, Microporous Mesoporous Mater. **174**, 211 (2015)
35. M. Nikoorazm, A. Ghorbani-Choghamarani, N. Noori, Appl. Organomet. Chem. **328**, 29 (2015)
36. M. Nikoorazm, A. Ghorbani-Choghamarani, N. Noori, J.. Porous Mater. (2015) in press
37. M.M. Lakouraj, M. Tajbakhsh, F. Shirini, M.V.A. Tamami, Synth. Commun. **775**, 35 (2005)
38. A. Shaabani, A. Bazgir, K. Soleimani, P. Salehi, Synth. Commun. **2935**, 33 (2003)
39. M. Abdo, Y. Zhan, V.L. Schramm, S. Knapp, Org. Lett. **2982**, 12 (2010)
40. Y. Inbushi, M. Yoshihara, Phosphorus Sulfur. **101**, 103 (1995)
41. F.R. Bisogno, A. Rioz-Martnez, C. Rodguez, I. Lavandera, G. de Gonzalo, T.E. Torres Pazmino, M.W. Fraaije, V. Gotor, Chem. Catal. **946**, 2 (2010)
42. A. Ghorbani-Choghamarani, G. Azadi, B. Tahmasbi, M. Hadizadeh-Hafshejani, Z. Abdi, Phosphorus Sulfur. **433**, 189 (2014)
43. A. Ghorbani-Choghamarani, H. Goudarziafshar, M. Nikoorazm, S. Yousefi, Lett. Org. Chem. **335**, 6 (2009)
44. A. Ghorbani-Choghamarani, S. Sardari, J. Sulfur Chem. **63**, 32 (2011)

45. A. Ghorbani-Choghmarani, M. Nikoorazm, H. Goudarziafshar, A. Shokr, H. Almasi, J. Chem. Sci. **453**, 123 (2011)
46. B. Karami, M. Montazerozohori, M.H. Habibi, Molecules **1358**, 10 (2005)
47. R. Das, D. Chakraborty, Tetrahedron Lett. **6255**, 51 (2010)
48. B. Karami, M. Montazerozohori, M. Moghadam, M.H. Habibi, Kh Niknam, Turk. J. Chem. **539**, 29 (2005)